Advances in Nano Research, *Vol. 9, No. 2 (2020) 91-104*
DOI: https://doi.org/10.12989/anr.2020.9.2.091

Frequency, bending and buckling loads of nanobeams with different cross sections

Ömer Civalek[1a], Büşra Uzun*[2] and M. Özgür Yaylı[2b]

[1]*China Medical University, Taichung, Taiwan*
[2]*Bursa Uludağ University, Faculty of Engineering, Department of Civil Engineering, Bursa, Turkey*

(*Received December 20, 2019, Revised July 4, 2020, Accepted July 7, 2020*)

Abstract. The bending, stability (buckling) and vibration response of nano sized beams is presented in this study based on the Eringen's nonlocal elasticity theory in conjunction with the Euler-Bernoulli beam theory. For this purpose, the bending, buckling and vibration problem of Euler-Bernoulli nanobeams are developed and solved on the basis of nonlocal elasticity theory. The effects of various parameters such as nonlocal parameter e_0a, length of beam L, mode number n, distributed load q and cross-section on the bending, buckling and vibration behaviors of carbon nanotubes idealized as Euler–Bernoulli nanobeam is investigated. The transverse deflections, maximum transverse deflections, vibrational frequency and buckling load values of carbon nanotubes are given in tables and graphs.

Keywords: bending; buckling; vibration; carbon nanotubes; finite element method; nonlocal elasticity theory; Euler-Bernoulli beam theory

1. Introduction

For the analysis of macro sized structural elements such as beam, plate, functionally graded plate various classical theories with various methods are used by researchers (Civalek and Kiracıoğlu 2007, Civalek and Acar 2007, Attia *et al*. 2018, Akgöz and Civalek 2011). The classical theories are sufficient to reflect the behaviors of macro sized structures and but these theories lose their validity when the dimensions are reduced.

Mechanical behaviors of micro/nano sized structures cannot be accurately explained with the classic continuum theory. Because of independent from the size, the formulation of classical continuum theory cannot capture the small size effect on micro/nano structures. In order to capture this effect which is important in understanding the behavior of nano / micro structures, length scales have been added to the constitutive equations of classical continuum mechanics. The most common of these theories are strain gradient theory (Mindlin 1965), couple stress theory (Toupin 1962, Mindlin and Tiersten 1962, Mindlin 1963, Koiter 1964), modified couple stress theory (Yang *et al*. 2002), modified strain gradient theory (Lam *et al*. 2003), nonlocal elasticity theory (Eringen 1983) and surface elasticity theory (Gurtin and Murdoch 1975a, b, 1978). These theories have been preferred by researchers for they help to understand the properties and behaviors of nano-sized structures more accurately.

In the literature, many studies have been performed using size-dependent continuum theories to determine the mechanical behaviors of small-size beams. Size-dependent buckling response of single walled carbon nanotubes (SWCNTs) was presented based on various beam theories in conjunction with modified strain gradient by Akgöz and Civalek (2017a). Demir and Civalek (2017a) developed a nonlocal finite element method for thermal vibration of simply-supported and clamped nanobeams on elastic matrix. Buckling analysis of silicon carbide nanotubes (SiCNTs) with different boundary conditions was given by Mercan and Civalek (2017) via the surface effect and nonlocal elasticity theories. In their paper, they used Euler-Bernoulli beam model and obtained the results using the harmonic differential quadrature method (HDQ). Dihaj *et al*. (2018) presented the effects of vibrational mode number, elastic medium and aspect ratio on the frequency transverse vibration of chiral DWCNTs. Uzun *et al*. (2020) investigated the vibration characteristics of functionally graded (FG) nanobeams with simply-supported boundary condition using non-local finite-element formulation. Also, Uzun and Yaylı (2020) presented the free vibration behaviors of Ti-6Al-4V/ZrO_2 FG nanobeam resting on Winkler–Pasternak elastic foundation in conjunction with Euler-Bernoulli beam and nonlocal elasticity theories. Ebrahimi and Salari (2015) presented thermal vibration response of SWCNTs embedded in an elastic foundation based on Reddy higher order shear deformation beam theory in conjunction with nonlocal elasticity theory. Free vibration response of non-homogeneous thick microbeams made of functionally graded materials was performed on the basis of hyperbolic shear deformation beam and modified

*Corresponding author, Ph.D. Student,
E-mail: buzun@uludag.edu.tr
[a] Ph.D. Professor, E-mail: omer@mail.cmuh.org.tw
[b] Ph.D. Associate Professor,
E-mail: ozguryayli@uludag.edu.tr

ISSN: 2287-237X (Print), 2287-2388 (Online)

couple stress theories by Akgöz and Civalek (2017b). In their paper, they investigated the effects of thermal and shear deformation on the vibrational behaviour of inhomogeneous microbeams made of FG material. Thermo-mechanical vibration of simply-supported SWCNTs embedded in an elastic medium was studied by Murmu and Pradhan (2009) on the basis of Euler Bernoulli beam and nonlocal elasticity theories. The influences of concentrated and distributed loads on the bending of the microbeam with various boundary conditions such as cantilever, clamped, propped cantilever and simply supported were investigated by Demir and Civalek (2017b) via Euler Bernoulli beam theory and the enhanced Eringen differential model. Ebrahimi and Nasirzadehby (2015) investigated the free vibration analysis of nanobeams on the basis of Eringen's nonlocal elasticity theory and Timoshenko beam theory which includes the effect of rotary inertia and shear deformation. In their paper, they used the differential transformation method (DTM) for solved the obtained equations. Murmu and Adhikari (2010) presented bending-vibration of prestressed SWCNT undergoing rotation via nonlocal elasticity theory and Euler-Bernoulli beam theory. Yaylı (2019) studied the thermal buckling of carbon nanotubes with rotational restraints in the framework Timoshenko beam theory and nonlocal beam theory. Thermal buckling loads are obtained using two Fourier infinite series with Stokes' transformation. Narendar and Gopalakrishnan (2009) presented the effect of nonlocal elasticity on the wave propagation in multi walled carbon nanotubes (MWCNTs). Aydoğdu and Arda (2016) investigated the torsional vibration response of double-walled carbon nanotubes (DWCNTs) in view of influences of some parameters such as van der Waals Force interaction, nonlocal parameter and nanotube length. In addition to these papers, size-dependent nonclassical analyzes of nanobeams and other nano / micro-scaled structures such as nano / microrod, nano / microshell, nano / microplate are widely available in the literature (Demir and Civalek 2013, Gürses *et al*. 2012, Numanoğlu *et al*. 2018, Narendar 2012, Wang *et al*. 2010, Ke *et al*. 2014, 2015, Heydarpour and Malekzadeh 2019, Akbaş 2019, Akgöz and Civalek 2014, Karličić *et al*. 2015, Asemi *et al*. 2014, Uzun and Civalek 2019a, b, Kong *et al*. 2008, Mokhtar *et al*. 2018, Yazid *et al*. 2018, Mercan *et al*. 2017, Numanoğlu and Civalek 2019, Youcef *et al*. 2018, Civalek and Demir 2011a, 2016, Semmah *et al*. 2019, Tounsi *et al*. 2013, Jalaei *et al*. 2018, 2019, Arani and Jalaei 2016, Jalaei and Arani 2018, Sahmani and Safaei 2019).

With the discovery of carbon nanotubes (Iijima 1991), a new era has initiated in the field of nanotechnology. Carbon nanotubes are one of the carbon allotropes and can be expressed simplistically as one-dimensional tube-shaped structures in nanometer dimensions. They are formed when the graphene sheet which is another carbon allotrope rolling on itself and takes the form of an open or closed cylinder. The structure which consists of the rolling of a single graphene layer is called single-walled carbon nanotube, while multiple interwoven tube structures refer to multi-walled carbon nanotubes. CNTs have novel properties such as high elastic modulus, high tensile properties, low density, conductivity or semiconductivity, effortlessly modifiability and great length-to-diameter ratio (Schrlau 2011, Uzun *et al*. 2018, Gopalakrishnan and Narendar 2013). Rapid developments in nanotechnology and the indicated superior properties of CNTs have induced to a significant acceleration in scientific studies to understand the mechanical behavior of nanoscale structures. As can be seen from previous studies in the literature, various analyzes of the behavior of nanotubes, especially CNTs (single-walled, double-walled or multi-walled) are a popular area of research for scientists and many other studies (Bedia *et al*. 2015, Civalek *et al*. 2020, Ece and Aydoğdu 2007, Barretta and Sciarra 2013, Reddy and Pang 2008, Ansari *et al*. 2011, Civalek and Demir 2011b, Yaylı 2016, 2017, 2018, Besseghier *et al*. 2015) are available.

Various analytical, semi-analytical and numerical methods can be used in the analysis of micro/nano structures. In the present paper, a detailed study is performed to investigate the bending, buckling (stability) and vibration responses of nano-scaled beams. Since carbon nanotubes are one-dimensional structures, it is common for CNTs to be modeled as structural elements like beams and rods in applications and continuum mechanics. In this study, carbon nanotube is modeled as simply-supported Euler-Bernoulli nanobeam. The influences of nonlocal parameter, length of beam, mode number, distributed load and cross-section on the bending, buckling and vibration behaviors of carbon nanotubes are examined.

2. Euler-Bernoulli beam theory

u_1, u_2 and u_3 are the displacements of the beam in the x (length), y (width), z (height) directions, respectively. w indicates transverse displacement of any point on the neutral axis. According to Euler–Bernoulli beam theory, the displacement field at any point may be described as Demir and Civalek (2017a), Reddy and Pang (2008).

$$u_1(x,z,t) = -z\frac{\partial w(x,t)}{\partial x}, \qquad u_2(x,z,t) = 0, \\ u_3(x,z,t) = w(x,t) \tag{1}$$

ε is the strain tensor and expressed for Euler-Bernoulli beam as follows.

$$\varepsilon_{ij} = 0.5(u_{i,j} + u_{j,i}) \tag{2}$$

Here $u_{i,j}$ means $u_{i,j} = \frac{\partial u_i}{\partial j}$.

We obtain from Eq. (2) the strains of the Euler-Bernoulli beam as follows.

$$\varepsilon_{xx} = -z\frac{\partial^2 w(x,t)}{\partial x^2}, \\ \varepsilon_{xy} = \varepsilon_{yx} = \varepsilon_{xz} = \varepsilon_{zx} = \varepsilon_{yy} = \varepsilon_{yz} = \varepsilon_{zy} = \varepsilon_{zz} = 0 \tag{3}$$

It is seen from the above equation that only ε_{xx} has a non-zero value. Stress σ for the linear elastic materials is expressed as follows.

$$\sigma = E\varepsilon \tag{4}$$

Here E is the elasticity modulus. σ_{xx} is obtained if ε_{xx} is written in Eq. (4) as we obtained in Eq. (3).

$$\sigma_{xx} = E\varepsilon_{xx} = -Ez\frac{\partial^2 w(x,t)}{\partial x^2} \tag{5}$$

Bending moment M and the moment of inertia I are given by

$$M = \int_A z\sigma_{xx}\, dA, I = \int_A z^2\, dA \tag{6}$$

Here, A is the cross-sectional area of the beam.

The Hamilton principle to be used to obtain equations of motion is expressed as follows (Reddy 2002).

$$\int_0^T (\delta T - \delta U + \delta W)\, dt = 0 \tag{7}$$

Where U, T and W are the strain energy, kinetic energy and work done by external loads, respectively. U, T and W for an element which has volume V and length L is as below.

$$U = \frac{1}{2}\int_V \sigma_{xx}\varepsilon_{xx} dV \tag{8}$$

$$T = \frac{1}{2}\int_V \rho\left(\frac{\partial w}{\partial t}\right)^2 dV \tag{9}$$

$$W = \frac{1}{2}\int_0^L \left(P\left(\frac{\partial w}{\partial x}\right)^2 + q(x)w(x)\right) dx \tag{10}$$

Here, ρ, P and q are the mass density, axial load and transverse uniform distributed load, respectively.

The first variation of the strain energy, kinetic energy and work done by external loads are obtained as follows.

$$\delta\int_0^T U dt = \int_0^T\int_0^L \left(-M\delta\left(\frac{\partial^2 w}{\partial x^2}\right)\right) dx dt \tag{11}$$

$$\delta\int_0^T T dt = \int_0^T\int_0^L \left(\rho A\frac{\partial w}{\partial t}\delta\left(\frac{\partial w}{\partial t}\right)\right) dx dt \tag{12}$$

$$\delta\int_0^T W dt = \int_0^T\int_0^L \left(P\frac{\partial w}{\partial x}\delta\left(\frac{\partial w}{\partial x}\right) + q\delta(w)\right) dx dt \tag{13}$$

Substituting Eqs. (11)-(13) into Eq. (7), we obtain the equilibrium equations from the Euler-Lagrange equation as follows.

$$\frac{\partial^2 M}{\partial x^2} = \rho A\frac{\partial^2 w}{\partial t^2} + P\frac{\partial^2 w}{\partial x^2} - q \tag{14}$$

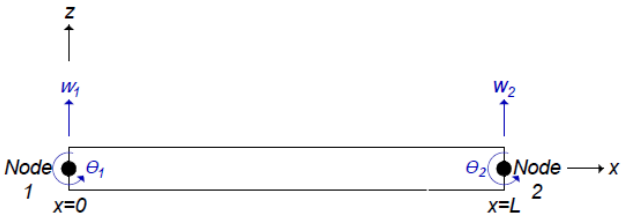

Fig. 1 A beam finite element

3. Nonlocal elasticity theory

In the classical continuum theories, stresses at a generic point depend only on the strains at that point. However, according to the nonlocal elasticity theory proposed by Eringen (1983), it is not enough to only know the strains at a generic point and strains at other points of the domain should be included in the formulas. The nonlocal constitutive relations of one dimensional case can be written as below (Eringen 1983, Reddy and Pang 2008)

$$\left(1 - (e_0 a)^2\frac{\partial^2}{\partial x^2}\right)\sigma_{xx} = E\varepsilon_{xx} \tag{15}$$

where $e_0 a$ is the nonlocal parameter. e_0 and a denote material constants which are determined experimentally and internal characteristic length, respectively.

Multiplying Eq. (15) by z and integrating over A, the nonlocal constitutive relation for Euler–Bernoulli nanobeam may be stated as

$$\int_A z\,\sigma dA - (e_0 a)^2\int_A z\frac{\partial^2\sigma}{\partial x^2} dA = \int_A z\, E\varepsilon dA \tag{16}$$

Substituting Eqs. (5) and (6) into (16), we obtain

$$M(x,t) - (e_0 a)^2\frac{\partial^2 M(x,t)}{\partial x^2} = -EI\frac{\partial^2 w(x,t)}{\partial x^2} \tag{17}$$

By differentiating Eq. (17) twice with respect to the variable x and substituting Eq. (14) into Eq. (17), we get the governing equation of Euler-Bernoulli nanobeam.

$$EI\frac{\partial^4 w(x,t)}{\partial x^4} - \frac{\partial^2}{\partial x^2}\left[(e_0 a)^2\rho A\frac{\partial^2 w(x,t)}{\partial t^2} + (e_0 a)^2 P\frac{\partial^2 w(x,t)}{\partial x^2} - (e_0 a)^2 q\right] + \cdots + \rho A\frac{\partial w^2(x,t)}{\partial t^2} + P\frac{\partial w^2(x,t)}{\partial x^2} q = 0 \tag{18}$$

4. Finite element formulation of nanobeam

The Euler-Bernoulli beam element is modelled using two nodes and two degrees of freedom per node. The degrees of freedom of a beam element are w_1 (displacement of node 1), θ_1 (rotation of node 1), w_2 (displacement of node 2), θ_2 (rotation of node 2) (Fig. 1). The shape function of the Euler-Bernoulli beam φ is

$$\varphi = \begin{Bmatrix} w_1 \\ \theta_1 \\ w_2 \\ \theta_2 \end{Bmatrix} = \begin{Bmatrix} \varphi_1 \\ \varphi_2 \\ \varphi_3 \\ \varphi_4 \end{Bmatrix} \tag{19}$$

Here φ_1, φ_2, φ_3 and φ_4 are expressed as below (Demir and Civalek 2017a, Uzun and Civalek 2019b).

$$\begin{aligned} &\varphi_1 = 1 - \frac{3x^2}{L^2} + \frac{2x^3}{L^3}, \varphi_2 = x - \frac{2x^2}{L} + \frac{x^3}{L^2}, \\ &\varphi_3 = \frac{3x^2}{L^2} - \frac{2x^3}{L^3}, \varphi_4 = -\frac{x^2}{L} + \frac{x^3}{L^2} \end{aligned} \tag{20}$$

In order to get the weak form of the governing equation of nonlocal Euler-Bernoulli beam, the residue R can be expressed as (Demir and Civalek 2017a).

$$\begin{aligned} R = {} & EI\frac{\partial^4 w(x,t)}{\partial x^4} - (e_0 a)^2 \frac{\partial^2}{\partial x^2}\left[\rho A \frac{\partial^2 w(x,t)}{\partial t^2}\right. \\ & \left. + P\frac{\partial^2 w(x,t)}{\partial x^2} - q\right] + \ldots + \rho A \frac{\partial w^2(x,t)}{\partial t^2} \\ & + P\frac{\partial w^2(x,t)}{\partial x^2} - q \end{aligned} \tag{21}$$

Eq. (21) is multiplied by a weighting function (φ) to specify the weighted residue. This weighting function is used as shape function (Demir and Civalek 2017a). When the weighted residual is integrated over the length.

$$\int_0^L \varphi R dx = 0 \tag{22}$$

Substituting Eq. (21) into Eq. (22)

$$\int_0^L \begin{bmatrix} \varphi EI\dfrac{\partial^4 w(x,t)}{\partial x^4} - \varphi(e_0 a)^2 \dfrac{\partial^2}{\partial x^2} \\ \left[\rho A \dfrac{\partial^2 w(x,t)}{\partial t^2} + P\dfrac{\partial^2 w(x,t)}{\partial x^2}\right] \\ + \ldots + \varphi\rho A \dfrac{\partial w^2(x,t)}{\partial t^2} + \varphi P \dfrac{\partial w^2(x,t)}{\partial x^2} \end{bmatrix} dx = 0 \tag{23}$$

Eq. (23) is integrated by parts. According to the chain rule, the general form.

$$\int_0^L \begin{bmatrix} EI\dfrac{\partial^2 \varphi}{\partial x^2}\dfrac{\partial^2 \varphi^T}{\partial x^2} - (e_0 a)^2 \rho A \dfrac{\partial \varphi}{\partial x}\dfrac{\partial \varphi^T}{\partial x}\ddot{w} \\ -(e_0 a)^2 P \dfrac{\partial^2 \varphi}{\partial x^2}\dfrac{\partial^2 \varphi^T}{\partial x^2} + \ldots \\ + \rho A \varphi \varphi^T \ddot{w} + P\dfrac{\partial \varphi}{\partial x}\dfrac{\partial \varphi^T}{\partial x} \end{bmatrix} dx = 0 \tag{24}$$

In Eq. (24), superscript T is the transpose operator. By using the shape functions in Eq. (20) and the dimensionless local coordinate, the bending stiffness matrix K_b, the classical and nonlocal geometric stiffness matrices K_G^c and K_G^{nl}, the classical and nonlocal mass matrices M^c and M^{nl} are obtained as follows.

$$K^b = EI\int_0^L \begin{Bmatrix} \varphi_1'' \\ \varphi_2'' \\ \varphi_3'' \\ \varphi_4'' \end{Bmatrix} \{\varphi_1'' \quad \varphi_2'' \quad \varphi_3'' \quad \varphi_4''\} dx \tag{25a}$$

$$= EI\int_0^L \begin{bmatrix} \varphi_1''\varphi_1'' & \varphi_1''\varphi_2'' & \varphi_1''\varphi_3'' & \varphi_1''\varphi_4'' \\ \varphi_2''\varphi_1'' & \varphi_2''\varphi_2'' & \varphi_2''\varphi_3'' & \varphi_2''\varphi_4'' \\ \varphi_3''\varphi_1'' & \varphi_3''\varphi_2'' & \varphi_3''\varphi_3'' & \varphi_3''\varphi_4'' \\ \varphi_4''\varphi_1'' & \varphi_4''\varphi_2'' & \varphi_4''\varphi_3'' & \varphi_4''\varphi_4'' \end{bmatrix} dx \tag{25b}$$

$$K^b = \frac{EI}{L^3}\begin{bmatrix} 12 & 6L & -12 & 6L \\ 6L & 4L^2 & -6L & 2L^2 \\ -12 & -6L & 12 & -6L \\ 6L & 2L^2 & -6L & 4L^2 \end{bmatrix} \tag{25c}$$

$$K_G^c = P\int_0^L \begin{Bmatrix} \varphi_1' \\ \varphi_2' \\ \varphi_3' \\ \varphi_4' \end{Bmatrix} \{\varphi_1' \quad \varphi_2' \quad \varphi_3' \quad \varphi_4'\} dx \tag{26a}$$

$$= P\int_0^L \begin{bmatrix} \varphi_1'\varphi_1' & \varphi_1'\varphi_2' & \varphi_1'\varphi_3' & \varphi_1'\varphi_4' \\ \varphi_2'\varphi_1' & \varphi_2'\varphi_2' & \varphi_2'\varphi_3' & \varphi_2'\varphi_4' \\ \varphi_3'\varphi_1' & \varphi_3'\varphi_2' & \varphi_3'\varphi_3' & \varphi_3'\varphi_4' \\ \varphi_4'\varphi_1' & \varphi_4'\varphi_2' & \varphi_4'\varphi_3' & \varphi_4'\varphi_4' \end{bmatrix} dx \tag{26b}$$

$$K_G^c = \frac{P}{30L}\begin{bmatrix} 36 & 3L & -36 & 3L \\ 3L & 4L^2 & -3L & -L^2 \\ -36 & -3L & 36 & -3L \\ 3L & -L^2 & -3L & 4L^2 \end{bmatrix} \tag{26c}$$

$$K_G^{nl} = (e_0 a)^2 P\int_0^L \begin{Bmatrix} \varphi_1'' \\ \varphi_2'' \\ \varphi_3'' \\ \varphi_4'' \end{Bmatrix} \{\varphi_1'' \quad \varphi_2'' \quad \varphi_3'' \quad \varphi_4''\} dx \tag{27a}$$

$$= (e_0 a)^2 P\int_0^L \begin{bmatrix} \varphi_1''\varphi_1'' & \varphi_1''\varphi_2'' & \varphi_1''\varphi_3'' & \varphi_1''\varphi_4'' \\ \varphi_2''\varphi_1'' & \varphi_2''\varphi_2'' & \varphi_2''\varphi_3'' & \varphi_2''\varphi_4'' \\ \varphi_3''\varphi_1'' & \varphi_3''\varphi_2'' & \varphi_3''\varphi_3'' & \varphi_3''\varphi_4'' \\ \varphi_4''\varphi_1'' & \varphi_4''\varphi_2'' & \varphi_4''\varphi_3'' & \varphi_4''\varphi_4'' \end{bmatrix} dx \tag{27b}$$

$$K_G^{nl} = \frac{(e_0 a)^2 P}{L^3}\begin{bmatrix} 12 & 6L & -12 & 6L \\ 6L & 4L^2 & -6L & 2L^2 \\ -12 & -6L & 12 & -6L \\ 6L & 2L^2 & -6L & 4L^2 \end{bmatrix} \tag{27c}$$

$$M^c = \rho A\int_0^L \begin{Bmatrix} \varphi_1 \\ \varphi_2 \\ \varphi_3 \\ \varphi_4 \end{Bmatrix} \{\varphi_1 \quad \varphi_2 \quad \varphi_3 \quad \varphi_4\} dx \tag{28a}$$

$$= \rho A\int_0^L \begin{bmatrix} \varphi_1\varphi_1 & \varphi_1\varphi_2 & \varphi_1\varphi_3 & \varphi_1\varphi_4 \\ \varphi_2\varphi_1 & \varphi_2\varphi_2 & \varphi_2\varphi_3 & \varphi_2\varphi_4 \\ \varphi_3\varphi_1 & \varphi_3\varphi_2 & \varphi_3\varphi_3 & \varphi_3\varphi_4 \\ \varphi_4\varphi_1 & \varphi_4\varphi_2 & \varphi_4\varphi_3 & \varphi_4\varphi_4 \end{bmatrix} dx \tag{28b}$$

$$M^c = \frac{\rho A}{420}\begin{bmatrix} 156L & 22L & 54L & -13L^2 \\ 22L^2 & 4L^3 & 13L^2 & -3L^3 \\ 54L & 13L^2 & 156L & -22L^2 \\ -13L^2 & -3L^2 & -22L^2 & 4L^3 \end{bmatrix} \tag{28c}$$

$$M^{nl} = (e_0a)^2\rho A\int_0^L \begin{Bmatrix}\varphi_1^{'}\\ \varphi_2^{'}\\ \varphi_3^{'}\\ \varphi_4^{'}\end{Bmatrix}\{\varphi_1^{'} \quad \varphi_2^{'} \quad \varphi_3^{'} \quad \varphi_4^{'}\}dx \tag{29a}$$

$$= (e_0a)^2\rho A\int_0^L \begin{bmatrix}\varphi_1^{'}\varphi_1^{'} & \varphi_1^{'}\varphi_2^{'} & \varphi_1^{'}\varphi_3^{'} & \varphi_1^{'}\varphi_4^{'}\\ \varphi_2^{'}\varphi_1^{'} & \varphi_2^{'}\varphi_2^{'} & \varphi_2^{'}\varphi_3^{'} & \varphi_2^{'}\varphi_4^{'}\\ \varphi_3^{'}\varphi_1^{'} & \varphi_3^{'}\varphi_2^{'} & \varphi_3^{'}\varphi_3^{'} & \varphi_3^{'}\varphi_4^{'}\\ \varphi_4^{'}\varphi_1^{'} & \varphi_4^{'}\varphi_2^{'} & \varphi_4^{'}\varphi_3^{'} & \varphi_4^{'}\varphi_4^{'}\end{bmatrix}dx \tag{29b}$$

$$M^{nl} = \frac{(e_0a)^2\rho A}{30L}\begin{bmatrix}36 & 3L & -36 & 3L\\ 3L & 4L^2 & -3L & -L^2\\ -36 & -3L & 36 & -3L\\ 3L & -L^2 & -3L & 4L^2\end{bmatrix} \tag{29c}$$

4.1 Finite element solution for buckling analysis

If we set the time derivative and q terms to zero in Eq. (18), we obtain the buckling equation of carbon nanotube as

$$EI\frac{\partial^4 w(x,t)}{\partial x^4} - (e_0a)^2\frac{\partial^2}{\partial x^2}\left[P\frac{\partial^2 w(x,t)}{\partial x^2}\right] + P\frac{\partial w^2(x,t)}{\partial x^2} = 0 \tag{30}$$

As can be seen from Eq. (30), when the following eigenvalue problem is solved, buckling loads of the Euler-Bernoulli nanobeam are obtained.

$$|K_b - \lambda K_G^t| = 0 \tag{31}$$

Here λ is buckling load of the beam. K_G^t is the total geometric stiffness matrix and given in Eq. (32).

$$K_G^t = K_G^c + K_G^{nl} \tag{32}$$

4.2 Finite element solution for vibration analysis

If we set the P and q terms equal to zero in Eq. (18), we obtain the vibration equation of carbon nanotubes as

$$EI\frac{\partial^4 w(x,t)}{\partial x^4} - (e_0a)^2\frac{\partial^2}{\partial x^2}\left[\rho A\frac{\partial^2 w(x,t)}{\partial t^2}\right] + \rho A\frac{\partial w^2(x,t)}{\partial t^2} = 0 \tag{33}$$

As can be seen from Eq. (33), when the following eigenvalue problem is solved, vibration frequencies of the Euler-Bernoulli nanobeam are obtained.

$$|K_b - \omega^2 M^t| = 0 \tag{34}$$

Here ω is circular frequency of the beam. M^t is the total mass matrix and given in Eq. (35).

$$M^t = M^c + M^{nl} \tag{35}$$

5. Solution for bending analysis

If we set the time derivative and P terms to zero in Eq. (18), we obtain the bending equation of carbon nanotube as

$$-EI\frac{\partial^4 w(x,t)}{\partial x^4} - (e_0a)^2\frac{\partial^2 q}{\partial x^2} = -q \tag{36}$$

Integrating Eq. (36), we obtain the following relations as (Reddy and Pang 2008).

$$V = -EI\frac{d^3 w}{dx^3} - (e_0a)^2\frac{dq}{dx} = -qx - c_1 \tag{37}$$

$$M = -EI\frac{d^2 w}{dx^2} - (e_0a)^2 q = -q\frac{x^2}{2} - c_1x - c_2 \tag{38}$$

$$EI\frac{dw}{dx} = -(e_0a)^2 qx + q\frac{x^3}{6} + c_1\frac{x^2}{2} + c_2x + c_3 \tag{39}$$

$$EIw = -(e_0a)^2 q\frac{x^2}{2} + q\frac{x^4}{24} + c_1\frac{x^3}{6} + c_2\frac{x^2}{2} + c_3x + c_4 \tag{40}$$

For a simply supported beam, at $x = 0$ and $x = L$ the boundary conditions are

$$w(x=0) = 0 \tag{41}$$

$$M(x=0) = 0 \tag{42}$$

$$w(x=L) = 0 \tag{43}$$

$$M(x=L) = 0 \tag{44}$$

Substituting boundary conditions into Eqs. (38) and (40), we obtain the transverse deflection and maximum transverse deflection as follows (Reddy and Pang 2008).

$$w(x) = \frac{qL^4}{24EI}\left[\left(\frac{x}{L}\right)^4 - 2\left(\frac{x}{L}\right)^3 + \frac{x}{L}\right] + \frac{(e_0a)^2 qL^2}{2EI}\left[\frac{x}{L} - \left(\frac{x}{L}\right)^2\right] \tag{45}$$

$$w\frac{qL^4}{384EI}\left[5 + 48\left(\frac{e_0a}{L}\right)^2\right]_{max} \tag{46}$$

6. Numerical results

In this section, effects of different parameters such as mode numbers, nonlocal parameters, distributed load and length of the beam on the bending, free vibration and buckling of carbon nanotubes are investigated. Several numerical examples are solved in order to points out to the possibility of enhancing or decreasing the bending, frequencies and buckling loads for different parameters. It should be noted that when the nonlocal parameter e_0a = 0, the results of classical elasticity theory are obtained. Carbon nanotubes are modeled as nanobeam and with simply supported boundary condition. Using the Eringen's nonlocal

Table 1 Mechanical and geometrical properties of carbon nanotubes

Mechanical properties*	Geometrical properties	
	Circular	Rectangular
young modulus, E = 1000 GPa density, ρ = 2300 kg/m^3	diameter, D = 1 nm area*, A = 0.785 nm^2 L = 20 nm	height, D = 1 nm width, b = 0.785 nm area, A = 0.785 nm^2 L = 20 nm

* (Reddy and Pang 2008)

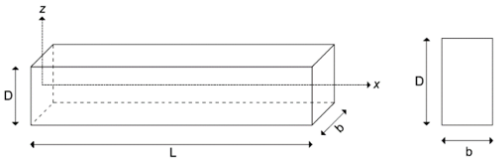

(a) Carbon nanotube with rectangular cross-section

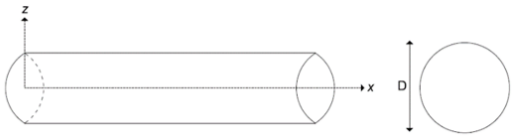

(b) Carbon nanotube with circular cross-section

Fig. 2 Illustration of carbon nanotube with circular cross-section

Table 3 First five buckling loads (nN) of circular nanotubes for various nonlocal parameters (L = 20 nm)

Mode number (n)	Circular cross-section e_0a (nm)				
	0.0	0.5	1.0	1.5	2.0
1	1.2112	1.2038	1.1820	1.1475	1.1024
2	4.8447	4.7281	4.4095	3.9644	3.4735
3	10.9006	10.3273	8.9198	7.2688	5.7728
4	19.3789	17.6381	13.8939	10.2628	7.5137
5	30.2796	26.2340	18.7275	12.6803	8.7326

Table 4 First five buckling loads (nN) of rectangular nanotubes for various nonlocal parameters (L = 20 nm)

Mode number (n)	Rectangular cross-section e_0a (nm)				
	0.0	0.5	1.0	1.5	2.0
1	1.6149	1.6050	1.5760	1.5300	1.4698
2	6.4596	6.3041	5.8794	5.2858	4.6313
3	14.5342	3.7697	11.8931	9.6917	7.6971
4	25.8386	23.5175	18.5251	13.6838	10.0183
5	40.3728	34.9786	24.9700	16.9071	11.6435

elasticity theory, Euler Bernoulli beam model is implemented. Two types of carbon nanotubes with circular and rectangular cross-section with same areas and height (diameter) are considered here to investigate their deflections, frequencies and buckling loads. Results for the two type carbon nanotubes are compared with each other. First, comparative examples are included to demonstrate the accuracy and convergence of the presented study. Mechanical and geometrical properties of carbon nanotubes are given in Table 1. Also, carbon nanotubes with different cross-section are illustrated in Fig. 2.

6.1 Buckling response of carbon nanotube

In this section, several tables and figures present the buckling loads for a carbon nanotube with different cross-section areas, nonlocal parameter and length. First, a comparative example is included to demonstrate the accuracy and convergence of the presented study buckling analysis of carbon nanotubes. Numerical results are shown by changing of the number of element N. Table 2 compares the results of the present finite element and the results presented by Aydoğdu (2009) for different nonlocal parameters. It is clear that there is a good agreement between the dimensionless critical buckling loads ($\bar{P}_{cr}$). In the following table $\mu = (e_0a)^2$.

The first five buckling load values obtained from the analyses of simply supported carbon nanotube for various nonlocal parameters ranging from 0 to 2 are presented in Tables 3 and 4. The buckling loads in Table 3 and 4 are calculated for carbon nanotube with circular and rectangular cross-section, respectively. It is seen from these tables, the buckling loads of carbon nanotube with rectangular cross-section are higher than the buckling loads of carbon nanotube with circular cross-section.

Variations of buckling loads of carbon nanotubes with

Table 2 Comparison of dimensionless critical buckling loads ($\bar{P}_{cr} = P_{cr}\frac{L^2}{EI}$) for simple supported case (L/h = 20)

μ (nm^2)	Aydoğdu (2009)	Present finite elemet method results							
		N = 7	N = 8	N = 9	N = 10	N = 11	N = 12	N = 13	N = 14
0	9.8696	9.8702	9.8699	9.8698	9.8697	9.8697	9.8697	9.8697	9.8696
1	9.6319	9.6325	9.6323	9.6320	9.6321	9.6320	9.6320	9.6320	9.6320
2	9.4055	9.4060	9.4058	9.4056	9.4056	9.4055	9.4055	9.4055	9.4055
3	9.1894	9.1899	9.1897	9.1896	9.1895	9.1895	9.1894	9.1894	9.1894
4	8.9830	8.9835	8.9833	8.9832	8.9831	8.9831	8.9831	8.9831	8.9830

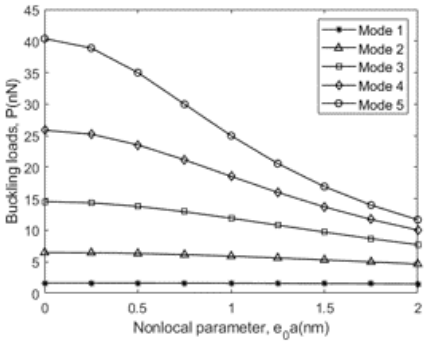

Fig. 3 The effects of nonlocal parameter on the buckling loads for different modes (rectangular, L = 20 nm)

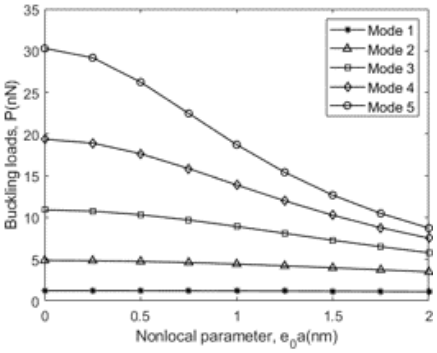

Fig. 4 The effects of nonlocal parameter on the buckling loads for different modes (circular, L = 20 nm)

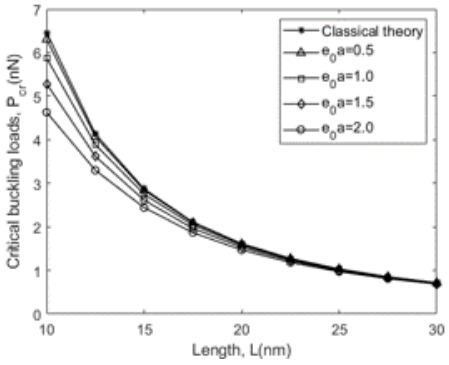

Fig. 5 The length effects on the critical buckling loads for different nonlocal parameters (rectangular)

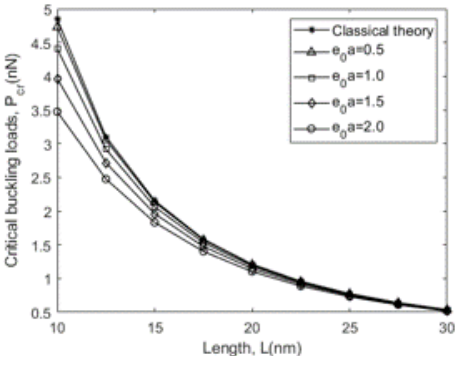

Fig. 6 The effects of length on the critical buckling loads for different nonlocal parameters (circular)

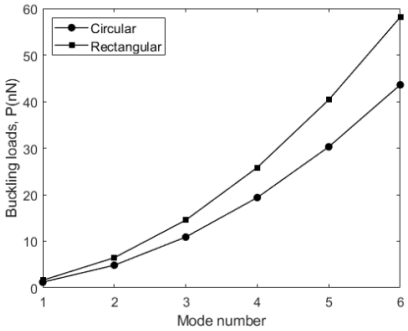

Fig. 7 The effects of mode number on the buckling loads (classical theory, L = 20 nm)

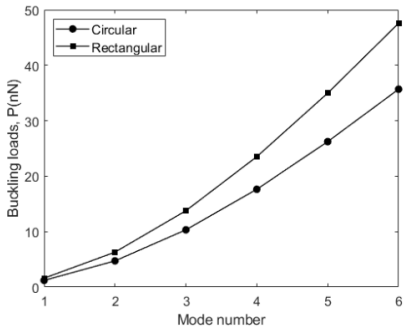

Fig. 8 The effects of mode number on the buckling loads ($e_{0}a$ = 0.5, L = 20 nm)

nonlocal parameter for the first five modes are shown in Figs. 3 and 4. It is seen from Figs. 3-4 that increase in the nonlocal parameter results in reduce in the buckling loads of the nanobeam. Also, it is obviously understood from the figure, nonlocal effects become more significant for higher modes.

Figs. 5 and 6 display the variation of critical buckling loads of CNTs with respect to length rise for various nonlocal parameter values. It is seen from Figs. 5 and 6 that by increasing the lengths, the critical buckling loads of the nanobeam decrease. Also, it is understood that nonlocal effects become more significant for lower lengths.

The effects of mode numbers to buckling loads of carbon nanotubes with circular and rectangular cross-sections are shown in Figs. 7 and 8. It is seen from these figures that increase in the mode numbers in enhance in the buckling loads of the nanobeam. Also, it is clearly seen that the buckling loads of carbon nanotube with rectangular coss-section are higher than the buckling loads of carbon nanotube with circular cross-section.

In Fig. 9, the variation of the critical buckling loads of carbon nanotubes with the change of nonlocal parameter and length are plotted. As stated before, it is clearly seen from this figure that the critical buckling loads decreased by increasing nonlocal parameter and length.

6.2 Vibration response of carbon nanotube

In this section, several tables and figures present the vibrational frequencies for a carbon nanotube with different cross-section areas, nonlocal parameter and length. First, a

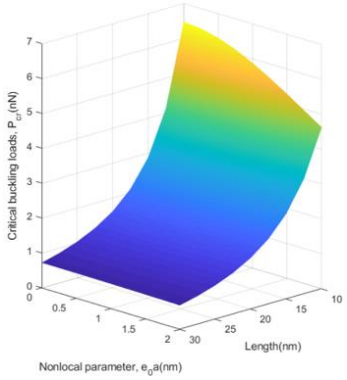

(a) rectangular

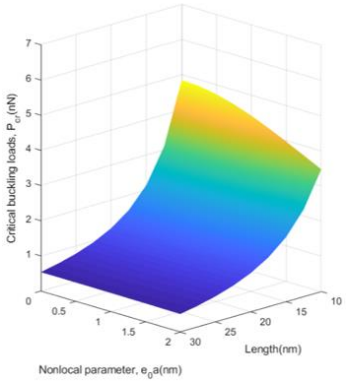

(b) circular

Fig. 9 The effects of length and nonlocal parameter on the critical buckling loads

comparative example is included to demonstrate the accuracy and convergence of the presented study for vibration analysis of carbon nanotubes. Numerical results are shown by changing of the number of element *N*. Table 5 compares the results of the present finite element and the results presented by Aydoğdu (2009) for different nonlocal parameters. It is clear that there is a good agreement between the dimensionless frequencies (ϖ). In the following table $\mu = (e_0 a)^2$.

The first five frequency values obtained from the analyses of simply supported carbon nanotube for various nonlocal parameters ranging from 0 to 2 are presented in Tables 6 and 7. The frequencies in Tables 6 and 7 are calculated for carbon nanotube with circular and rectangular cross-section, respectively. It is seen from these tables, the vibrational frequencies of carbon nanotube with rectangular cross-section are higher than the frequencies of carbon nanotube with

Table 6 First five frequencies (10^9 rad/s) of nanotubes for various nonlocal parameters (L = 20 nm)

Mode number (n)	Circular cross-section e_0a (nm)				
	0.0	0.5	1.0	1.5	2.0
1	128.6222	128.2273	127.0641	125.1939	122.7092
2	514.4887	508.2565	490.8367	465.4023	435.6346
3	1157.5996	1126.7455	1047.1551	945.2868	842.4167
4	2057.9548	1963.3469	1742.5383	1497.6297	1281.4411
5	3215.5544	2993.0431	2528.8377	2080.8779	1726.8469

Table 7 First five frequencies (10^9 rad/s) of nanotubes for various nonlocal parameters (L = 20 nm)

Mode number (n)	Rectangular cross-section e_0a (nm)				
	0.0	0.5	1.0	1.5	2.0
1	148.5201	148.0641	146.7210	144.5615	141.6924
2	594.0804	586.8841	566.7694	537.4002	503.0275
3	1336.6808	1301.0537	1209.1505	1091.5232	972.7390
4	2376.3215	2267.0778	2012.1099	1729.3138	1479.6807
5	3713.0024	3456.0684	2920.0503	2402.7909	1993.9910

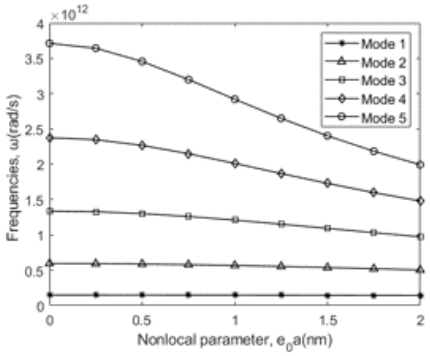

Fig. 10 The effects of nonlocal parameter on the frequencies for different modes (rectangular, L = 20 nm)

circular cross-section.

Variations of vibrational frequencies of carbon nanotube with nonlocal parameter for the first five modes are shown

Table 5 Comparison of dimensionless frequencies ($\varpi = \omega L^2 \sqrt{\frac{\rho A}{EI}}$) for simple supported case (L/h = 20)

μ (nm^2)	Aydoğdu (2009)	Present finite elemet method results							
		N = 7	N = 8	N = 9	N = 10	N = 11	N = 12	N = 13	N = 14
0	9.8696	9.8699	9.8698	9.8697	9.8697	9.8696	9.8696	9.8696	9.8696
1	9.7498	9.7503	9.7502	9.7502	9.7501	9.7501	9.7501	9.7501	9.7501
2	9.6343	9.6350	9.6349	9.6348	9.6348	9.6348	9.6348	9.6348	9.6348
3	9.5228	9.5237	9.5236	9.5235	9.5235	9.5235	9.5235	9.5234	9.5234
4	9.4150	9.4161	9.4160	9.4160	9.4159	9.4159	9.4159	9.4159	9.4159

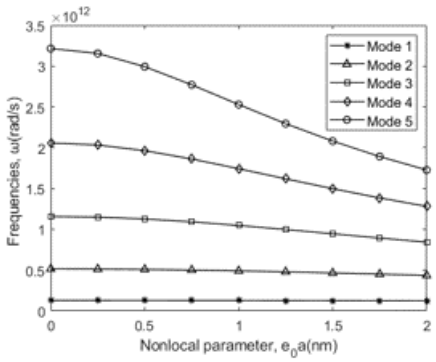

Fig. 11 The effects of nonlocal parameter on the frequencies for different modes (circular, L = 20 nm)

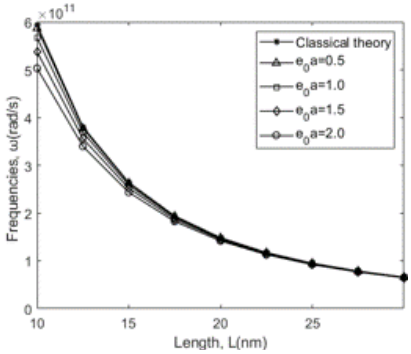

Fig. 12 The effects of length on the frequencies for different nonlocal parameters (rectangular, mode 1)

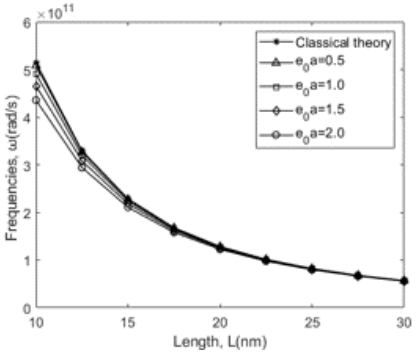

Fig. 13 The effects of length on the frequencies for different nonlocal parameters (circular, mode 1)

in Figs. 10 and 11. It is seen from Figs. 10-11 that increase in the nonlocal parameter results in reduce in the frequencies of the nanobeam. Also, it is seen from the figure, effects of nonlocal parameter become more prominent for higher modes.

Figs. 12 and 13 depict the variation of frequencies of CNTs with respect to length rise for the classical and nonlocal elasticity theory. It is observed from Figs. 12-13 that by increasing the lengths, the frequencies of the nanobeam decrease. In addition, it is concluded from the figures that nonlocal effects become more significant for lower lengths.

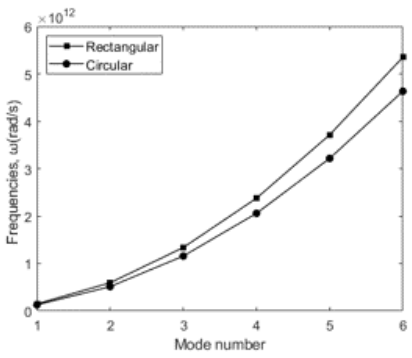

Fig. 14 The effects of mode number on the frequencies (classical theory, L = 20 nm)

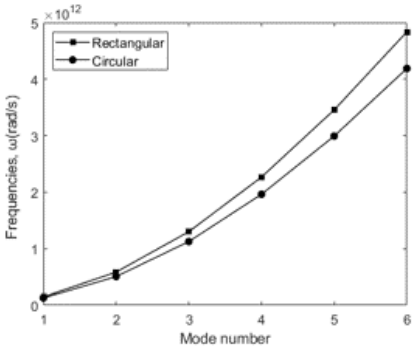

Fig. 15 The effects of mode number on the frequencies (e_0a = 0.5, L = 20 nm)

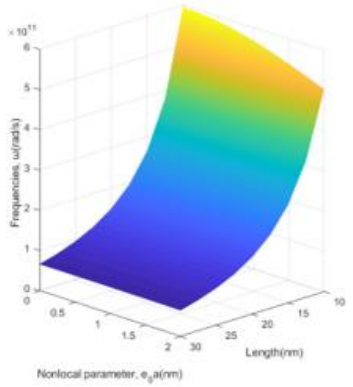

(a) rectangular

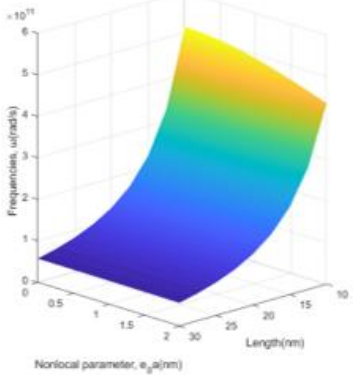

(b) circular

Fig. 16 The effects of length and nonlocal parameter on the frequencies

Table 8 Maximum deflections (nm) of circular nanotubes for various nonlocal parameters and distributed loads (L = 20 nm)

q (nN/nm)	Circular cross-section e_0a (nm)				
	0.0	0.5	1.0	1.5	2.0
0.01	0.4244	0.4270	0.4346	0.4473	0.4652
0.02	0.8488	0.8539	0.8692	0.8947	0.9303
0.03	1.2732	1.2809	1.3038	1.3420	1.3955
0.04	1.6977	1.7078	1.7384	1.7893	1.8606
0.05	2.1221	2.1348	2.1730	2.2367	2.3258

Table 9 Maximum deflections (nm) of rectangular nanotubes for various nonlocal parameters and distributed loads (L = 20 nm)

q (nN/nm)	Rectangular cross-section e_0a (nm)				
	0.0	0.5	1.0	1.5	2.0
0.01	0.3183	0.3202	0.3259	0.3355	0.3489
0.02	0.6366	0.6404	0.6519	0.6710	0.6977
0.03	0.9549	0.9607	0.9778	1.0065	1.0466
0.04	1.2732	1.2809	1.3038	1.3420	1.3955
0.05	1.5915	1.6011	1.6297	1.6775	1.7443

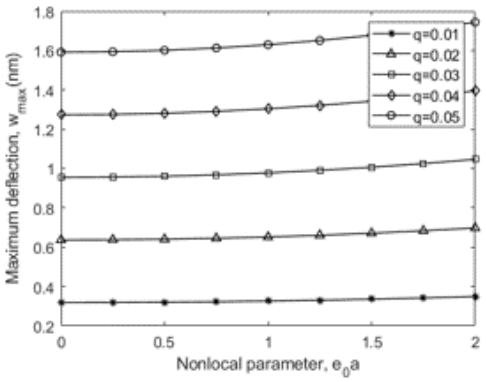

Fig. 17 The effects of nonlocal parameter on the maximum deflections for different uniform distributed loads (rectangular, L = 20 nm)

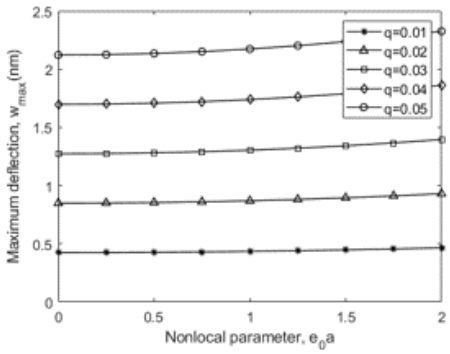

Fig. 18 The effects of nonlocal parameter on the maximum deflections for different uniform distributed loads (circular, L = 20 nm)

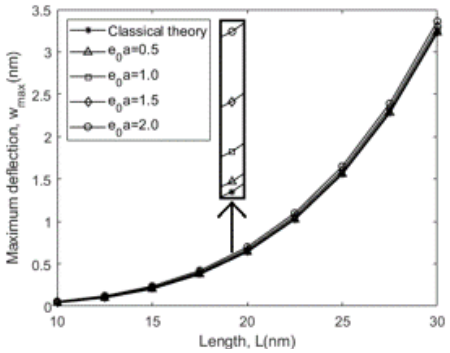

Fig. 19 The effects of length on the maximum deflections for different nonlocal parameters (rectangular, q = 0.02 nN/nm)

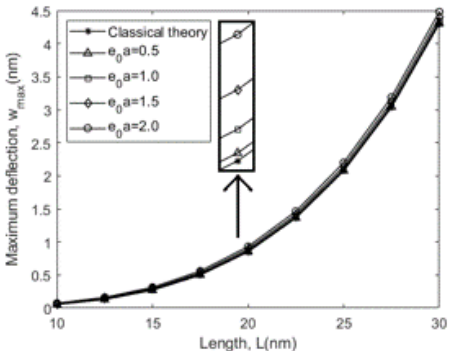

Fig. 20 The effects of length on the maximum deflections for different nonlocal parameters (circular, q = 0.02 nN/nm)

Figs. 14 and 15 illustrate the variation of frequencies of carbon nanotubes versus mode numbers for rectangular and circular cross-sections. Based on the results in Figs. 14-15 the increasing mode numbers leads to an increase in the values of frequencies. It is also said that the frequencies of carbon nanotube with rectangular cross-section are higher than the frequencies of carbon nanotube with circular cross-section.

To demonstrate the effects of the nonlocal parameters and lengths of nanobeam on the frequencies, variation of natural frequencies is plotted in Fig. 16. As stated before, it is clearly seen from this figure that the frequencies decreased by increasing nonlocal parameter and length.

6.3 Bending response of carbon nanotubes

In this section, several tables (Tables 8-9) and figures (Figs. 17-23) present the bending response for a carbon nanotube with different cross-section areas, nonlocal parameter, distributed load and length.

The maximum deflection values obtained from the analyses of simply supported carbon nanotube under uniform distributed load for various nonlocal parameters

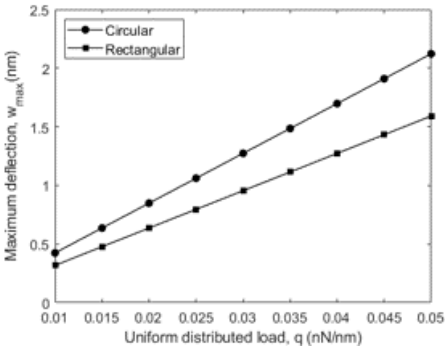

Fig. 21 The effects of uniform distributed loads on the maximum deflections (classical theory, L = 20 nm)

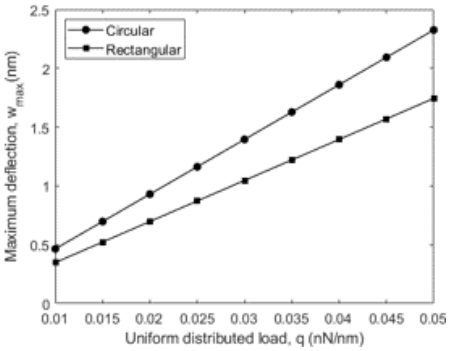

Fig. 22 The effects of uniform distributed loads on the maximum deflections (e_0a = 2, L = 20 nm)

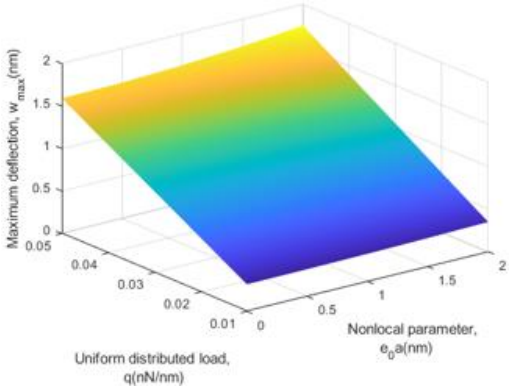

(a) rectangular

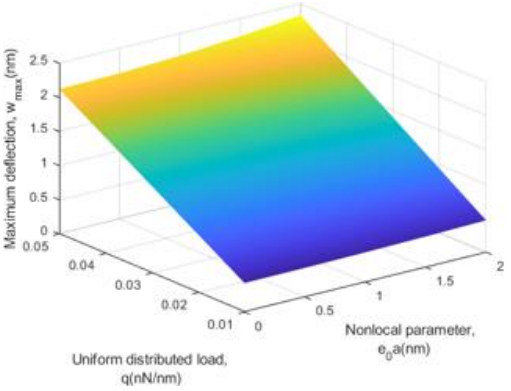

(b) circular

Fig. 23 The effects of distributed load and nonlocal parameter on the maximum deflection

ranging from 0 to 2 are presented in Tables 8 and 9. The maximum deflections in Tables 8 and 9 are calculated for carbon nanotubes with circular and rectangular cross-section, respectively. It is seen from these tables, the maximum deflections of carbon nanotube with circular cross-section are higher than the frequencies of carbon nanotube with rectangular cross-section.

Variations of maximum deflections of carbon nanotubes with nonlocal parameter for various uniform distributed loads are shown in Figs. 17 and 18. It is seen from Figures 17-18 that increase in the nonlocal parameter results in increase in the maximum deflections of the nanobeam.

Figs. 19 and 20 depict the variation of maximum deflections of carbon nanotubes with respect to length rise for the classical and nonlocal elasticity theories. It is observed from Figs. 19-20 that by increasing the lengths, the maximum deflections of the nanobeam increase.

Figs. 21 and 22 illustrate the variation of maximum deflections of carbon nanotubes versus uniform distributed loads for rectangular and circular cross-sections. Based on the results in Figs. 21-22, the increasing uniform distributed loads leads to an increase in the values of maximum deflections. It is also seen that the deflections of carbon nanotube with circular cross-section are higher than the deflections of carbon nanotube with rectangular cross-section.

To demonstrate the effects of the nonlocal parameters and uniform distributed loads of nanobeam on the deflections, variation of maximum deflections is plotted in Fig. 23. As stated before, it is clearly seen from this figure that the deflections increased by increasing nonlocal parameter and distributed loads.

7. Conclusions

In present study, the bending, stability (buckling) and vibration analyzes of simply supported nanobeams are researched using Eringen's nonlocal elasticity theory. Euler-Bernoulli beam theory is used to simulate the bending, buckling and vibration response of nanobeam. Several numerical examples are solved to point out effects of nonlocal parameter, length, uniform distributed load and cross-section on the bending, buckling and vibration of the nanobeam. The most significant results obtained take into consideration numerical studies can be summarized as follows: Similar results are obtained in buckling and vibration analyzes of carbon nanotubes. The natural frequencies and buckling loads for a rectangular nanobeam are higher than that for the corresponding circular nanobeam. The height and cross-sectional area values are kept equal for both type carbon nanotubes. The moment of inertia of the rectangular carbon nanotube has a greater value. For this reason, the frequency and buckling values of the rectangular cross-section nanotube are higher than the frequency and buckling values of the circular cross-section nanotube. As the lengths of carbon nanotubes become increaser the values of frequency and buckling load

decrease. Similarly, increment of nonlocal effects results in decrease the values of frequency and buckling load. The maximum deflection values for a rectangular nanobeam are lower than that for the corresponding circular nanobeam. As the lengths of carbon nanotubes become increaser the values of deflection values increase. Similarly, increment of nonlocal effects results in increase the values of deflection. Also, the increasing uniform distributed load leads to an increase in the values of maximum deflections.

References

Akbaş, Ş.D. (2019), "Axially forced vibration analysis of cracked a nanorod", *J. Comput. Appl. Mech.*, **50**(1), 63-68. https://doi.org/10.22059/jcamech.2019.281285.392.

Akgoz, B. and Civalek, O. (2011), "Nonlinear vibration analysis of laminated plates resting on nonlinear two-parameters elastic foundations", *Steel Compos. Struct., Int. J.*, **11**(5), 403-421. https://doi.org/10.12989/scs.2011.11.5.403.

Akgöz, B. and Civalek, Ö. (2014), "Longitudinal vibration analysis for microbars based on strain gradient elasticity theory", *J. Vib. Control*, **20**(4), 606-616. https://doi.org/10.1177/1077546312463752.

Akgöz, B. and Civalek, Ö. (2017a), "A size-dependent beam model for stability of axially loaded carbon nanotubes surrounded by Pasternak elastic foundation", *Compos. Struct.*, **176**, 1028-1038. https://doi.org/10.1016/j.compstruct.2017.06.039.

Akgöz, B. and Civalek, Ö. (2017b), "Effects of thermal and shear deformation on vibration response of functionally graded thick composite microbeams", *Compos. Part B Eng.*, **129**, 77-87. https://doi.org/10.1016/j.compositesb.2017.07.024.

Ansari, R. Gholami, R. and Darabi, M.A. (2011), "Thermal buckling analysis of embedded single-walled carbon nanotubes with arbitrary boundary conditions using the nonlocal Timoshenko beam theory", *J. Therm. Stresses*, **34**(12), 1271-1281. https://doi.org/10.1080/01495739.2011.616802.

Arani, A.G. and Jalaei, M.H. (2016), "Transient behavior of an orthotropic graphene sheet resting on orthotropic visco-Pasternak foundation", *Int. J. Eng. Sci.*, **103**, 97-113. https://doi.org/10.1016/j.ijengsci.2016.02.006.

Asemi, S.R. Farajpour, A. Asemi, H.R. and Mohammadi, M. (2014), "Influence of initial stress on the vibration of double-piezoelectric-nanoplate systems with various boundary conditions using DQM", *Physica E Low Dimens. Syst. Nanostruct.*, **63**, 169-179. https://doi.org/10.1016/j.physe.2014.05.009.

Attia, A. Bousahla, A.A., Tounsi, A., Mahmoud, S.R. and Alwabli, A.S. (2018), "A refined four variable plate theory for thermoelastic analysis of FGM plates resting on variable elastic foundations", *Struct. Eng. Mech., Int. J.*, **65**(4), 453-464. https://doi.org/10.12989/sem.2018.65.4.453.

Aydogdu, M. (2009), "A general nonlocal beam theory: its application to nanobeam bending, buckling and vibration", *Physica E Low Dimens. Syst. Nanostruct.*, **41**(9), 1651-1655. https://doi.org/10.1016/j.physe.2009.05.014.

Aydogdu, M. and Arda, M. (2016), "Torsional vibration analysis of double walled carbon nanotubes using nonlocal elasticity", *Int. J. Mech. Mater. Des.*, **12**(1), 71-84. https://doi.org/10.1007/s10999-014-9292-8.

Barretta, R. and Marotti de Sciarra, F. (2013), "A nonlocal model for carbon nanotubes under axial loads", *Adv. Mater. Sci. Eng.*, 360935. https://doi.org/10.1155/2013/360935.

Bedia, W.A., Benzair, A., Semmah, A., Tounsi, A. and Mahmoud, S.R. (2015), "On the thermal buckling characteristics of armchair single-walled carbon nanotube embedded in an elastic medium based on nonlocal continuum elasticity", *Braz. J. Phys.*, **45**(2), 225-233. https://doi.org/10.1007/s13538-015-0306-2.

Besseghier, A., Heireche, H., Bousahla, A.A., Tounsi, A. and Benzair, A. (2015), "Nonlinear vibration properties of a zigzag single-walled carbon nanotube embedded in a polymer matrix", *Adv. Nano Res., Int. J.*, **3**(1), 29-37. https://doi.org/10.12989/anr.2015.3.1.029.

Civalek, Ö. and Acar, M.H. (2007), "Discrete singular convolution method for the analysis of Mindlin plates on elastic foundations", *Int. J. Press. Vessel. Pip.*, **84**(9), 527-535. https://doi.org/10.1016/j.ijpvp.2007.07.001.

Civalek, Ö. and Demir, Ç. (2011a), "Bending analysis of microtubules using nonlocal Euler–Bernoulli beam theory", *Appl. Math. Model.*, **35**(5), 2053-2067. https://doi.org/10.1016/j.apm.2010.11.004.

Civalek, Ö. and Demir, C. (2011b), "Buckling and bending analyses of cantilever carbon nanotubes using the euler-bernoulli beam theory based on non-local continuum model", *Asian J. Civ. Eng.*, **12**(5), 651-661.

Civalek, Ö. and Demir, C. (2016), "A simple mathematical model of microtubules surrounded by an elastic matrix by nonlocal finite element method", *Appl. Math. Comput.*, **289**, 335-352. https://doi.org/10.1016/j.amc.2016.05.034.

Civalek, Ö. and Kiracioglu, O. (2007), "Discrete singular convolution for free vibration analysis of anisotropic rectangular plates", *Math. Comput. Appl.*, **12**(3), 151-160. https://doi.org/10.3390/mca12030151.

Civalek, Ö., Uzun, B., Yaylı, M.Ö. and Akgöz, B. (2020), "Size-dependent transverse and longitudinal vibrations of embedded carbon and silica carbide nanotubes by nonlocal finite element method", *Eur. Phys. J. Plus*, **135**(4), 381. https://doi.org/10.1140/epjp/s13360-020-00385-w.

Demir, Ç. and Civalek, Ö. (2013), "Torsional and longitudinal frequency and wave response of microtubules based on the nonlocal continuum and nonlocal discrete models", *Appl. Math. Model.*, **37**(22), 9355-9367. https://doi.org/10.1016/j.apm.2013.04.050.

Demir, Ç. and Civalek, Ö. (2017a), "A new nonlocal FEM via Hermitian cubic shape functions for thermal vibration of nano beams surrounded by an elastic matrix", *Compos. Struct.*, **168**, 872-884. https://doi.org/10.1016/j.compstruct.2017.02.091.

Demir, Ç. and Civalek, Ö. (2017b), "On the analysis of microbeams", *Int. J. Eng. Sci*, **121**, 14-33. https://doi.org/10.1016/j.ijengsci.2017.08.016.

Dihaj, A., Zidour, M., Meradjah, M., Rakrak, K., Heireche, H. and Chemi, A. (2018), "Free vibration analysis of chiral double-walled carbon nanotube embedded in an elastic medium using non-local elasticity theory and Euler Bernoulli beam model", *Struct. Eng. Mech., Int. J.*, **65**(3), 335-342. https://doi.org/10.12989/sem.2018.65.3.335.

Ebrahimi, F. and Nasirzadeh, P. (2015), "A nonlocal Timoshenko beam theory for vibration analysis of thick nanobeams using differential transform method", *J. Theor. Appl. Mech.*, **53**(4), 1041-1052. https://doi.org/10.15632/jtam-pl.53.4.1041.

Ebrahimi, F. and Salari, E. (2015), "Thermo-mechanical vibration analysis of a single-walled carbon nanotube embedded in an elastic medium based on higher-order shear deformation beam theory", *J. Mech. Sci. Technol.*, **29**(9), 3797-3083. https://doi.org/10.1007/s12206-015-0826-2.

Ece, M.C. and Aydogdu, M. (2007), "Nonlocal elasticity effect on vibration of in-plane loaded double-walled carbon nano-tubes", *Acta Mechanica*, **190**(1-4), 185-195. https://doi.org/10.1007/s00707-006-0417-5.

Eringen, A.C. (1983), "On differential equations of nonlocal elasticity and solutions of screw dislocation and surface waves",

J. Appl. Phys., **54**, 4703-4710. https://doi.org/10.1063/1.332803.
Gopalakrishnan, S. and Narendar, S. (2013), *Wave Propagation in Nanostructures: Nonlocal Continuum Mechanics Formulations*, Springer International Publishing, Switzerland.
Gurtin, M.E. and Murdoch, A.I. (1975a), "Addenda to our paper: A continuum theory of elastic material surfaces*", Arch. Ration. Mech. Anal*., **59**(4), 389-390. https://doi.org/10.1007/BF00250426.
Gurtin, M.E. and Murdoch, A.I. (1975b), "A continuum theory of elastic material surfaces", *Arch. Ration. Mech. Anal.,* **57**(4), 291-323. https://doi.org/10.1007/BF00261375.
Gurtin, M.E. and Murdoch, A.I. (1978), "Surface stress in solids", *Int. J. Solids Struct.,* **14**(6), 431-440. https://doi.org/10.1016/0020-7683(78)90008-2.
Gürses, M., Akgöz, B. and Civalek, Ö. (2012), "Mathematical modeling of vibration problem of nano-sized annular sector plates using the nonlocal continuum theory via eight-node discrete singular convolution transformation", *Appl. Math. Comput.*, **219**(6), 3226-3240. https://doi.org/10.1016/j.amc.2012.09.062.
Heydarpour, Y. and Malekzadeh, P. (2019), "Dynamic stability of cylindrical nanoshells under combined static and periodic axial loads", *J. Braz. Soc. Mech. Sci. Eng*., **41**(4), 184. https://doi.org/10.1007/s40430-019-1675-1.
Iijima, S. (1991), "Helical microtubules of graphitic carbon", *Nature*, **354**(6348), 56. https://doi.org/10.1038/354056a0.
Jalaei, M.H. and Arani, A.G. (2018), "Size-dependent static and dynamic responses of embedded double-layered graphene sheets under longitudinal magnetic field with arbitrary boundary conditions", *Compos. Part B Eng*., **142**, 117-130. https://doi.org/10.1016/j.compositesb.2017.12.053.
Jalaei, M.H., Arani, A.G. and Tourang, H. (2018), "On the dynamic stability of viscoelastic graphene sheets", *Int. J. Eng. Sci*., **132**, 16-29. https://doi.org/10.1016/j.ijengsci.2018.07.002.
Jalaei, M.H., Arani, A.G. and Nguyen-Xuan, H. (2019), "Investigation of thermal and magnetic field effects on the dynamic instability of FG Timoshenko nanobeam employing nonlocal strain gradient theory", *Int. J. Mech. Sci*., **161**, 105043. https://doi.org/10.1016/j.ijmecsci.2019.105043.
Karličić, D., Cajić, M., Murmu, T. and Adhikari, S. (2015), "Nonlocal longitudinal vibration of viscoelastic coupled double-nanorod systems", *Eur. J. Mech. A Solids*, **49**, 183-196. https://doi.org/10.1016/j.euromechsol.2014.07.005.
Ke, L.L., Wang, Y.S., Yang, J. and Kitipornchai, S. (2014), "The size-dependent vibration of embedded magneto-electro-elastic cylindrical nanoshells", *Smart Mater. Struct.*, **23**(12), 125036. https://doi.org/10.1088/0964-1726/23/12/125036.
Ke, L.L., Liu, C. and Wang, Y.S. (2015), "Free vibration of nonlocal piezoelectric nanoplates under various boundary conditions", *Physica E Low Dimens. Syst. Nanostruct.*, **66**, 93-106. https://doi.org/10.1016/j.physe.2014.10.002.
Koiter, W.T. (1964), "Couple stresses in the theory of elasticity: I and II", *Proc. K. Ned. Akad. Wet. B Phys. Sci*., **67**, 17-44.
Kong, S., Zhou, S., Nie, Z. and Wang, K. (2008), "The size-dependent natural frequency of Bernoulli–Euler micro-beams", *Int. J. Eng. Sci.*, **46**(5), 427-437. https://doi.org/10.1016/j.ijengsci.2007.10.002.
Lam, D.C.C., Yang, F., Chong, A.C.M., Wang, J. and Tong, P. (2003), "Experiments and theory in strain gradient elasticity", *J. Mech. Phys. Solids*, **51**(8), 1477-1508. https://doi.org/10.1016/S0022-5096(03)00053-X.
Mercan, K. and Civalek, Ö. (2017), "Buckling analysis of silicon carbide nanotubes (SiCNTs) with surface effect and nonlocal elasticity using the method of HDQ", *Compos. Part B Eng*., **114**, 34-45. https://doi.org/10.1016/j.compositesb.2017.01.067.
Mercan, K., Numanoglu, H.M., Akgöz, B., Demir, C. and Civalek, Ö. (2017), "Higher-order continuum theories for buckling response of silicon carbide nanowires (SiCNWs) on elastic matrix", *Arch. Appl. Mech*., **87**(11), 1797-1814. https://doi.org/10.1007/s00419-017-1288-z.
Mindlin, R.D. (1963), "Influence of couple-stresses on stress concentrations", *Exp. Mech*., **3**(1), 1-7. https://doi.org/10.1007/BF02327219.
Mindlin, R.D. (1965), "Second gradient of strain and surface-tension in linear elasticity", *Int. J. Solids Struct*., **1**(4), 417-438. https://doi.org/10.1016/0020-7683(65)90006-5.
Mindlin, R.D. and Tiersten, H.F. (1962), "Effects of couple-stresses in linear elasticity", *Arch. Ration. Mech. Anal.,* **11**, 415-448. https://doi.org/10.1007/BF00253946.
Mokhtar, Y., Heireche, H., Bousahla, A.A., Houari, M.S.A., Tounsi, A. and Mahmoud, S.R. (2018), "A novel shear deformation theory for buckling analysis of single layer graphene sheet based on nonlocal elasticity theory", *Smart Struct. Syst., Int. J*., **21**(4), 397-405. https://doi.org/10.12989/sss.2018.21.4.397.
Murmu, T. and Adhikari, S. (2010), "Scale-dependent vibration analysis of prestressed carbon nanotubes undergoing rotation", *J. Appl. Phys*., **108**(12), 123507. https://doi.org/10.1063/1.3520404.
Murmu, T. and Pradhan, S.C. (2009), "Thermo-mechanical vibration of a single-walled carbon nanotube embedded in an elastic medium based on nonlocal elasticity theory", *Comput. Mater. Sci.*, **46**(4), 854-859. https://doi.org/10.1016/j.commatsci.2009.04.019.
Narendar, S. and Gopalakrishnan, S. (2009), "Nonlocal scale effects on wave propagation in multi-walled carbon nanotubes", *Comput. Mater. Sci.,* **47**(2), 526-538. https://doi.org/10.1016/j.commatsci.2009.09.021.
Narendar, S. (2012), "Spectral finite element and nonlocal continuum mechanics based formulation for torsional wave propagation in nanorods", *Finite Elem. Anal. Des.,* **62**, 65-75. https://doi.org/10.1016/j.finel.2012.06.012.
Numanoğlu, H.M. and Civalek, Ö. (2019), "On the dynamics of small-sized structures", *Int. J. Eng. Sci*., **145**, 103164. https://doi.org/10.1016/j.ijengsci.2018.05.001.
Numanoğlu, H.M., Akgöz, B. and Civalek, Ö. (2018), "On dynamic analysis of nanorods", *Int. J. Eng. Sci*., **130**, 33-50. https://doi.org/10.1016/j.ijengsci.2018.05.001.
Reddy, J.N. (2002), *Energy Principles and Variational Methods in Applied Mechanics*, John Wiley & Sons, USA.
Reddy, J.N. and Pang, S.D. (2008), "Nonlocal continuum theories of beams for the analysis of carbon nanotubes", *J. Appl. Phys*., **103**(2), 023511. https://doi.org/10.1063/1.2833431.
Sahmani, S. and Safaei, B. (2019), "Nonlinear free vibrations of bi-directional functionally graded micro/nano-beams including nonlocal stress and microstructural strain gradient size effects", *Thin Wall. Struct.,* **140**, 342-356. https://doi.org/10.1016/j.tws.2019.03.045.
Schrlau, M.G. (2011), "Carbon nanotube-based sensors: overview", *Compr. Biomater*., **3**, 519-528.
Semmah, A., Heireche, H., Bousahla, A.A. and Tounsi, A. (2019), "Thermal buckling analysis of SWBNNT on Winkler foundation by non local FSDT", *Adv. Nano Res., Int. J*., **7**(2), 89-98. https://doi.org/10.12989/anr.2019.7.2.089.
Tounsi, A., Benguediab, S., Semmah, A. and Zidour, M. (2013), "Nonlocal effects on thermal buckling properties of double-walled carbon nanotubes", *Adv. Nano Res., Int. J*., **1**(1), 1-11. https://doi.org/10.12989/anr.2013.1.1.001.
Toupin, R.A. (1962), "Elastic materials with couple-stresses", *Arch. Ration. Mech. Anal*., **11**(1), 385-414. https://doi.org/10.1007/BF00253945.
Uzun, B., Numanoglu, H. and Civalek, O. (2018), "Free vibration analysis of BNNT with different cross-Sections via nonlocal

FEM", *J. Comput. Appl. Mech.*, **49**(2), 252-260. https://doi.org/10.22059/jcamech.2018.

Uzun, B. and Civalek, Ö. (2019a), "Nonlocal FEM formulation for vibration analysis of nanowires on elastic matrix with different materials", *Math. Comput. Appl.*, **24**(2), 38. https://doi.org/10.3390/mca24020038.

Uzun, B. and Civalek, Ö. (2019b), "Free vibration analysis silicon nanowires surrounded by elastic matrix by nonlocal finite element method", *Adv. Nano Res., Int. J.*, **7**(2), 99-108. https://doi.org/10.12989/anr.2019.7.2.099.

Uzun, B. and Yaylı, M.Ö. (2020), "Nonlocal vibration analysis of Ti-6Al-4V/ZrO_2 functionally graded nanobeam on elastic matrix", *Arab. J. Geosci.*, **13**(4), 1-10. https://doi.org/10.1007/s12517-020-5168-4.

Uzun, B., Yaylı, M.Ö. and Deliktaş, B. (2020), "Free vibration of FG nanobeam using a finite-element method", *Micro Nano Lett.*, **15**(1), 35-40. https://doi.org/10.1049/mnl.2019.0273.

Wang, Y.Z., Li, F.M. and Kishimoto, K. (2010), "Scale effects on flexural wave propagation in nanoplate embedded in elastic matrix with initial stress", *Appl. Phys. A*, **99**(4), 907-911. https://doi.org/10.1007/s00339-010-5666-4.

Yang, F., Chong, A.C.M., Lam, D.C.C. and Tong, P. (2002), "Couple stress based strain gradient theory for elasticity", *Int. J. Solids Struct.*, **39**(10), 2731-2743. https://doi.org/10.1016/S0020-7683(02)00152-X.

Yayli, M.Ö. (2016), "A compact analytical method for vibration analysis of single-walled carbon nanotubes with restrained boundary conditions", *J. Vib. Control*, **22**(10), 2542-2555. https://doi.org/10.1177/1077546314549203.

Yayli, M.Ö. (2017), "Buckling analysis of a cantilever single-walled carbon nanotube embedded in an elastic medium with an attached spring", *Micro Nano Lett.*, **12**(4), 255-259. https://doi.org/10.1049/mnl.2016.0662.

Yayli, M.Ö. (2018), "On the torsional vibrations of restrained nanotubes embedded in an elastic medium", *J. Braz. Soc. Mech. Sci. Eng.*, **40**(9), 419. https://doi.org/10.1007/s40430-018-1346-7.

Yayli, M.Ö. (2019), "Effects of rotational restraints on the thermal buckling of carbon nanotube", *Micro Nano Lett.*, **14**(2), 158-162. https://doi.org/10.1049/mnl.2018.5428.

Yazid, M., Heireche, H., Tounsi, A., Bousahla, A.A. and Houari, M.S.A. (2018), "A novel nonlocal refined plate theory for stability response of orthotropic single-layer graphene sheet resting on elastic medium", *Smart Struct. Syst., Int. J.*, **21**(1), 15-25. https://doi.org/10.12989/sss.2018.21.1.015.

Youcef, D.O., Kaci, A., Benzair, A., Bousahla, A.A. and Tounsi, A. (2018), "Dynamic analysis of nanoscale beams including surface stress effects", *Smart Struct. Syst., Int. J.*, **21**(1), 65-74. https://doi.org/10.12989/sss.2018.21.1.065.